THE ROYAL SOCIETY

High-resolution characterization of microdefects by X-ray diffuse scattering

By Jerzy Gronkowski, Janusz Borowski and Elżbieta Zielińska-Rohozińska

Institute of Experimental Physics, University of Warsaw, Hoża 69, 00-681 Warsaw, Poland

Highly tellurium-doped GaAs samples were investigated by high-resolution X-ray diffractometry in the triple-axis mode. Different reciprocal maps, depending on the technological process, are presented and interpreted as caused by different microdefects. Computer simulations allow us to determine the type of microdefects, namely the orthorhombic defects and dislocations loops. A theoretical approach for defects composed of several atoms is proposed. Alternative descriptions of pairs of defects as uniform distributions of such paired defects or non-uniform distributions of single-defect components are presented.

Keywords: GaAs; defects; correlation function; cluster expansion

1. Introduction

In the present paper an application of X-ray high-resolution diffractometry to defect characterization is described. The method consists of a very good collimation and monochromatization of the beam incident on a sample and the use of an analyser crystal to extract a well-collimated beam from the scattered radiation, containing information on the defects present in the sample. From angular scans of the sample and analyser, intensity maps of the beam in reciprocal space are obtained; these maps allow us to characterize the defects.

Defects of very different types are generated during the growth and technological processes (i.e. thermal annealing) of the crystals. The knowledge of these types of defects is very important for the quality optimization of the materials. As a non-destructive method, X-ray diffractometry is very convenient in this respect. It can be complemented by X-ray topography (Lang 1957, 1959) to show defects of larger sizes.

It is known (Fuller & Wolfstrin 1963; Słupiński *et al*. 1996; Zielińska-Rohozińska *et al*. 1997; Borowski *et al*. 1998) that thermal annealing modifies significantly the free-electron concentration of very highly doped n-GaAs. It also leads to creation of certain types of extended defects. Results concerning the effect of thermal annealing of heavily doped GaAs:Te on diffuse X-ray scattering have previously been reported (Słupiński *et al*. 1996; Zielińska-Rohozińska *et al*. 1997). Small defects (with radii smaller than 0.1 μm) are created in these samples, depending on the concentration of Te atoms. It is interesting to note that the content of such microdefects can be substantially reduced using a suitable annealing process.

In this paper various defects are analysed, some of them consisting of several or several tens of atoms only. Subsequent phases of dislocation-loop formation and the corresponding changes in the maps are also discussed.

2. Theoretical basis

(*a*) *Point and extended defects*

A theoretical model of X-ray diffraction in real crystals, containing randomly distributed defects which deform the crystal lattice, should be based on a statistical description of the whole system. In the diffraction process an X-ray is scattered in part by the atoms inside the defects, and partly by the deformed lattice outside the defects. The measured total intensity is compared with the theoretically calculated mean intensity, averaged over the statistical ensemble of crystals which are macroscopically identical, but differ through their microscopic distributions of defects.

Atoms forming the defects (e.g. donors) may be single and isolated or grouped in precipitate clusters of given geometrical shapes, e.g. spheres or dislocation loops (Larson & Schmatz 1974), depending on their concentration and the technological processes to which the crystals are subjected. It is convenient to use the term *single-atom defects* for the former and the term *many-atom defects* for the latter. On the other hand, if the effects arising due to the scattering inside a defect are not measured or even not measurable, it is sufficient to describe the lattice displacements around the defect as a displacement field of a *point defect*. Such a field is most conveniently obtained by extrapolation of the outer displacement field on the inner region of the defect. For example, if a spherical inclusion is characterized by the following displacement field:

$$\boldsymbol{t}(\boldsymbol{r}) = \begin{cases} A\boldsymbol{r}, & \text{for } r \leqslant R, \\ AR^3 \dfrac{\boldsymbol{r}}{r^3}, & \text{for } r \geqslant R, \end{cases} \tag{2.1}$$

where A and R are constants (the misfit parameter and the 'size' of the inclusion, respectively), $\boldsymbol{r}$ is the position vector and r is its length, then such an extrapolation consists of substituting (2.1) by the corresponding point-defect displacement field:

$$\boldsymbol{t}_{\mathrm{p}}(\boldsymbol{r}) = AR^3 \frac{\boldsymbol{r}}{r^3}, \quad r \neq 0. \tag{2.2}$$

At the same time it is hard to determine the contribution of the scattering on the inner region of defects (Trinkaus 1971), especially of small dimension ($R < 1\,\mu\mathrm{m}$), because it would require precise measurements of the far wings of the rocking curves, which depend on the structure of the defect cores.

The difference between the point defects and extended defects is analogous as in the description of electrons or protons usually applied in electrodynamics. If only the trajectories of these particles in cloud chambers are measured, then they can be sufficiently and naturally described as point-like objects. However, if one wants to investigate the magnetic dipole moment of an electron (Wesley & Rich 1970; Levine & Wright 1971), its internal structure cannot be neglected. For the purpose of this article it may be therefore concluded that a single-atom defect should be treated as being extended if the scattering by this atom is observed, and, similarly, a defect

which is *ca.* 1 μm large can be treated as a point defect if the scattering by its core is neither observed nor described.

If an object is treated as a point defect, then not only can the continuous displacement field (2.1) be replaced by the tempered distribution (2.2), but also the density $f_k(\boldsymbol{r})$ of the volume force exerted by the defect on the crystal lattice may be described by a tempered distribution (Borowski 1998):

$$f_k(\boldsymbol{r}) = -P_{kj}\frac{\partial}{\partial x^j}\delta(\boldsymbol{r}), \tag{2.3}$$

where P_{kj} is the so-called double-force tensor of the defect (Trinkaus 1972) and $\delta(\boldsymbol{r})$ is the Dirac delta distribution.

(*b*) *The correlation functions*

As mentioned in § 2 *a*, the measured intensity of the diffuse scattering is compared with the theoretical intensity averaged over the statistical ensemble of crystals with different microscopic defect distributions, expressed through the mean values, correlation functions and higher-order moments (which have not been taken into account in the existing descriptions of X-ray diffuse scattering). It is therefore essential to formulate precisely what is meant by 'mean values' and 'correlation functions' as well as to define the relations between these two quantities in the expressions appearing in the models of diffuse scattering, e.g. in the so-called cluster expansion (Kubo 1962).

For the definition of the defect volume concentration $\rho(\boldsymbol{r})$, a characteristic volume V_0 is chosen, such that $V_0 \gg L^3 \gg R^3$, where L is the mean distance between the defects and R is their mean size; at the same time $V_0 \ll V$, where V is the whole crystal volume. The number N of defects in the volume V_0 around the point $\boldsymbol{r}$ is then by definition $N(\boldsymbol{r}) = \rho(\boldsymbol{r})V_0$ (with the approximation to statistical fluctuations). Obviously, in some cases ρ may be taken in the crystal as position dependent.

The non-normalized correlation functions of random variables $\{x_1, \ldots, x_n\}$ with the overall distribution of the probability density $f(x_1, \ldots, x_n)$ are defined here as

$$\varepsilon(x_i, x_j) = \langle x_i x_j\rangle - \langle x_i\rangle\langle x_j\rangle, \tag{2.4}$$

where

$$\langle x_i\rangle = \int \mathrm{d}x_1 \cdots \mathrm{d}x_n\, f(x_1, \ldots, x_n)x_i \tag{2.5}$$

and

$$\langle x_i x_j\rangle = \int \mathrm{d}x_1 \cdots \mathrm{d}x_n\, f(x_1, \ldots, x_n)x_i x_j. \tag{2.6}$$

If the variables x_i and x_j are independent, then $\langle x_i x_j\rangle = \langle x_i\rangle\langle x_j\rangle$ and $\varepsilon(x_i, x_j) = 0$. However, it is important to note that the reverse relation is not always true and $\varepsilon(x_i, x_j) = 0$ does not necessarily mean that x_i and x_j are independent (Feller 1961). Therefore, it should be remembered that the correlation function (2.4) represents only an indirect measure of independence of variables; normally x_i and x_j for which $\varepsilon(x_i, x_j)$ is zero are called unconnected or uncorrelated (and *not* independent) variables.

The degree of correlation of defect distributions can be determined taking, in particular, $x_i = \rho(\boldsymbol{r}_i)$. As an example consider a non-uniform distribution of defects with a constant concentration, such that each defect can be either isolated (i.e. there are no other defects within distance L) or defects can form crystallographically oriented pairs (i.e. for a defect situated at $\boldsymbol{r}_0$ there is a closest neighbour at, say, $\boldsymbol{r}_0 + \frac{1}{10}L[110]$, where [110] is an exemplary orientation of the pair). Denoting by I_i the number of isolated defects in the regions of volume V_0 surrounding the points $\boldsymbol{r}_i$ $(i = 1, 2)$, and by P_i the number of the exemplary defect pairs in the same regions, the condition of constant concentration can be written as $I_1 + 2P_1 = I_2 + 2P_2$. However, generally $P_1 \neq P_2$ and statistical distributions of such pairs can be described by defining the suitable random variables and their correlation functions. Examples of such random variables are $u(\boldsymbol{r})$ and $v(\boldsymbol{r})$, defined in the following way: $u(\boldsymbol{r}) = 1$ when there is a defect at $\boldsymbol{r}$ and $u(\boldsymbol{r}) = 0$ when there is no defect there; $v(\boldsymbol{r}) = 1$ when there is a defect at $\boldsymbol{r} + \frac{1}{10}L[110]$ and $v(\boldsymbol{r}) = 0$ when there is no defect there.

(*c*) *The cumulant function*

In order to obtain theoretically the intensity of X-ray diffuse scattering from a crystal with statistically distributed microdefects, the quantities of the following type must be calculated:

$$F = \left\langle \exp\left\{ \sum_{i=1}^{N} a_i C_i \right\} \right\rangle, \tag{2.7}$$

where C_i are random variables connected with the distributions of defects, while the functions a_i represent the displacement field of the defect. Expression (2.7) can be calculated when it is written in a somewhat different form:

$$\left\langle \exp\left\{ \sum_{i=1}^{N} a_i C_i \right\} \right\rangle = \exp\{K(a_1, \ldots, a_N)\}, \tag{2.8}$$

and the so-called cumulant function K is sought when both sides of (2.8) are expanded in the Taylor series and compared (Kubo 1962). The expression for the cumulant function can be obtained by grouping first the terms containing only a_i, then pairs $\{a_i, a_j\}$, up to the terms containing all functions $\{a_i, \ldots, a_N\}$:

$$K(a_1, \ldots, a_N) = \sum_{i=1}^{N} K_1(a_i) + \sum_{i,j=1}^{N} K_2(a_i, a_j) + \cdots + K_N(a_1, \ldots, a_N). \tag{2.9}$$

This is the so-called cluster expansion (Kubo 1962), and the functions K_i can be expressed by the statistical moments of the distributions of the random variables c_i. If a subset $\{c_{i_1}, \ldots, c_{i_m}\}$ of the independent random variables can be found, then their function $K_m(a_{i_1}, \ldots, a_{i_m}) = 0$ and the corresponding term is removed from series (2.9).

(*d*) *Application to X-ray diffuse scattering*

In physical applications it is rather difficult to estimate how many terms in (2.9) are sufficient for a good approximation of the cumulant function K. Some terms can

be chosen in an heuristic way and then one can verify if the next terms are only small corrections. In calculations for X-ray diffuse scattering, normally only the first term in (2.9) remains for defects' uniform distributions, or the two first terms for non-uniform distributions. Therefore, a sufficient approximation for expressions like (2.8) is (Kubo 1962; Krivoglaz 1984; Kaganer *et al*. 1997)

$$\left\langle \exp\left\{\sum_{i=1}^{N} a_i C_i\right\}\right\rangle \cong \sum_{i=1}^{N} \log\{1 + a_1\langle c_i\rangle\} + \sum_{i,j=1}^{N} \log\left\{1 + a_i a_j \frac{\langle c_i c_j\rangle - \langle c_i\rangle\langle c_j\rangle}{(1 + a_i\langle c_i\rangle)(1 + a_j\langle c_j\rangle)}\right\}. \tag{2.10}$$

The expression in the denominator of the second term represents the correlation function of the random variables, describing the presence of defects in the possible positions (in the discrete notation used here) or the defects' volume-concentration correlation function (in the continuous notation).

For most applications to X-ray diffuse scattering by statistically distributed microdefects, expression (2.10) has proven to be sufficiently accurate. However, theoretically it may happen that the defects' distribution is such that they exist only in threes, so that each group of three lies at a distance of all others far larger than the distances within each group. Then three first terms in (2.9) would have to be taken into account.

(*e*) *The intensity of scattered diffuse radiation*

In the case of X-ray diffuse scattering by microdefects the measured intensity is compared with the following theoretical expression (Dederichs 1971; Krivoglaz 1984):

$$I_{\mathrm{D}}(\boldsymbol{Q}) = \sum_{k,l} \exp\{\mathrm{i}\boldsymbol{Q}\cdot(\boldsymbol{R}_k - \boldsymbol{R}_l)\} \times \{\langle\exp[\mathrm{i}\boldsymbol{Q}\cdot(\boldsymbol{u}_k - \boldsymbol{u}_l)]\rangle - \langle\exp[\mathrm{i}\boldsymbol{Q}\cdot\boldsymbol{u}_k]\rangle\langle\exp[\mathrm{i}\boldsymbol{Q}\cdot\boldsymbol{u}_l]\rangle\}, \tag{2.11}$$

where $\boldsymbol{Q} = \boldsymbol{K}_h - \boldsymbol{K}_0$, $\boldsymbol{R}_k$ is the position of the kth atom in the mean lattice and $\boldsymbol{u}_k$ is the deviation of the kth atom from $\boldsymbol{R}_k$.

Averaging in (2.11) is done by the method described in § 2 *b* (for details, see Krivoglaz 1984; Kaganer *et al*. 1997). Intensity is calculated (for a uniform distribution of defects) with only the first term in (2.9), i.e. the correlation functions are neglected. The full expressions in this case are given elsewhere (formulae (4)–(10) in Borowski *et al*. (1998)). The intensity I_{m} measured in a triple-axis experiment is a sum of two terms: (i) a term due to diffraction in an ideal monochromator, sample and analyser crystals, described by reflectivities R_{m}, R_{s}, and R_{a}, respectively (Holý & Mikulik 1996); and (ii) a term due to diffraction in the (ideal) crystals described by R_{m} and R_{a} as well as the effect of microdefects described by I_{D}. This can be symbolically written as

$$I_{\mathrm{m}} = R_{\mathrm{m}} * R_{\mathrm{s}} * R_{\mathrm{a}} + R_{\mathrm{m}} * I_{\mathrm{D}} * R_{\mathrm{a}}, \tag{2.12}$$

where the symbol $*$ means a repeated operation of integrating over beam divergences and the spectral distribution of the incident beam.

Table 1. *The annealing processes of the four samples of LEC Te-doped 001-oriented GaAs slices studied in this paper*

(Q stands for quenching, n[Te] means the tellurium concentration.)

sample S1	As-grown	$n[\mathrm{Te}] = 4.5 \times 10^{18}$ cm^{-3}
sample S2	(i) 1195 °C for 2 h + Q (ii) 1100 °C for 5 h + Q (iii) 1180 °C for 2.5 h + Q	$n[\mathrm{Te}] = 1.0 \times 10^{19}$ cm^{-3}
sample S3	950 °C for 66 h + Q	$n[\mathrm{Te}] = 6.0 \times 10^{18}$ cm^{-3}
sample S4	755 °C for 139 h	$n[\mathrm{Te}] = 1.5 \times 10^{19}$ cm^{-3}

3. Experimental

The four samples studied in the present work were LEC Te-doped 001-oriented slices of GaAs. The last three were subjected to the annealing processes detailed in table 1.

High-resolution X-ray diffraction reciprocal space maps were measured using a Philips MRD diffractometer set for 440 germanium reflections with Cu-$K\alpha 1$ radiation. Figure 1*a* presents a map of sample S1; the characteristic streaks are seen—the vertical sample streak and the skew analyser streak. This image can be treated as a reference map for the perfect crystal as the sample apparently contained only native defects (Zielińska-Rohozińska *et al*. 1997). Tellurium atoms form single-atom defects which cause a weak deformation of the neighbouring GaAs lattice; as a result the value of I_{D} is small. In such a case the second term in (2.12) is much smaller than the first term, and the map is described by the first term, giving the characteristic streaks (Holý & Mikulik 1996).

Figure 1*b* presents a map of sample S2, resembling somewhat the streaks of figure 1*a*, but blown up and deformed, especially in the centre of the map. The technological process to which the sample was subjected has led to defect formation (either clustering of Te atoms, or formation of some defects composed of Ga and As atoms, due to the presence of Te atoms, or both). In this case the value of I_{D} is greater than in the former case, but still relatively small (small concentration of defects and/or small deformation of the bulk GaAs lattice). Both terms in (2.12) are comparable. A quantitative analysis of such maps is difficult, because the influence of the defects on the map characteristics is limited to some deformation of the streaks.

The map of figure 1*c* (for large values of q) presents a picture characteristic of dislocation loops (sample S3) with the Burgers vector $\boldsymbol{b} = \frac{1}{3}[111]$ and the unit vector $\boldsymbol{n}$ normal to the plane of the loop being parallel to $\boldsymbol{b}$. The image for small q seen in figure 1*c* cannot be treated as being caused by these loops. Two possibilities can be envisaged. First, the concentration of the loops can be so small that the second term in (2.12) is still rather small and for small values of q (but greater than a few half-widths of the Bragg peak where the kinematical approximation is valid) the Bragg scattering has comparable intensity with the diffuse scattering. In this case one should calculate the total intensity rather than separate it into the diffuse and Bragg scattering terms. On the other hand, for large values of q the diffuse scattering is dominant and the characteristic loop image (simulation shown in figure 1*d*) is clearly visible. Secondly, other defects may be present whose image is dominant for small values of q and less visible for larger q.

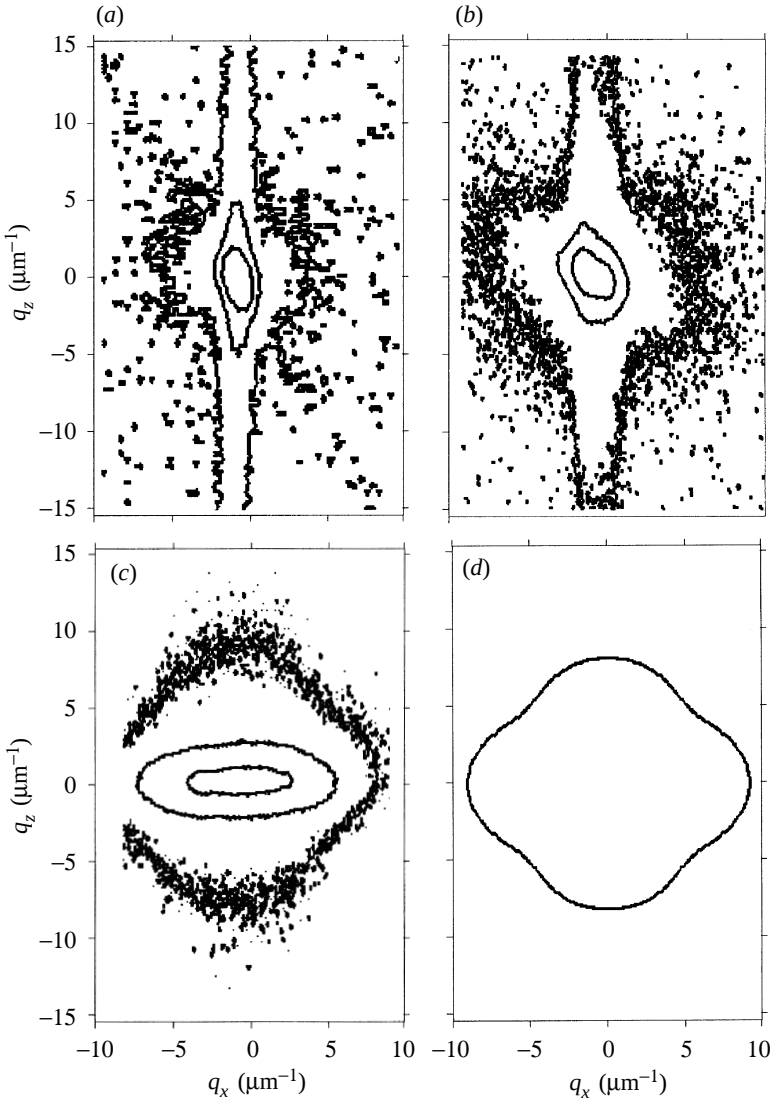

Figure 1. Diffuse scattering maps of the GaAs samples: (*a*) almost ideal map (streak, sample S1); (*b*) map with very small diffuse intensity (deformed streak, sample S2); (*c*) map showing the presence of dislocation loops (sample S3) $\boldsymbol{b} = \frac{1}{3}[111]$; (*d*) simulation for dislocation loops of figure 1*c*. The intensity levels shown are 1.5 counts per second (cps, outer contour), 80 cps (middle contour) and 800 cps (inner contour).

The maps of figure 1*a–c* can be treated as an illustration of the dislocation-loop formation process as an effect of various technological processes. At the same time they illustrate the characteristics of the maps as a function of diffuse scattering intensity: a streak when I_{D} is very small (figure 1*a*); a deformed streak when I_{D} is comparable with the Bragg scattering intensity (figure 1*b*); and an image of the defects (at least for greater q) when I_{D} is dominant. In the latter case the expressions for R_{m} and R_{a} in the second term of (2.12) define only the resolution of the experiment.

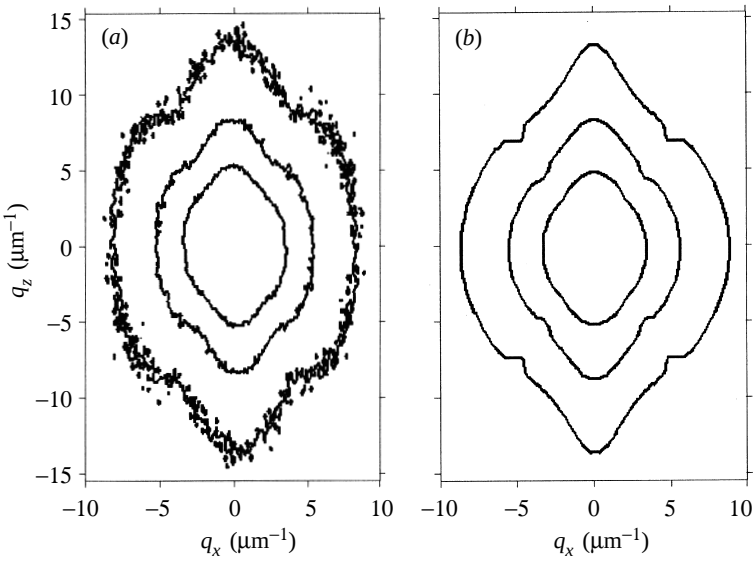

Figure 2. (*a*) Symmetrized experimental map for sample S4, $\boldsymbol{h} = [004]$; (*b*) corresponding simulation for the orthorhombic defects. The intensity levels shown are 10 cps (outer contour), 50 cps (middle contour) and 200 cps (inner contour).

Figure 2*a* shows symmetrized diffuse intensity for sample S4, while figure 2*b* presents a theoretical simulation for defects of orthorhombic symmetry (Borowski 1997; Borowski *et al*. 1998). They may be formed by [110]-oriented pairs of donor atoms (or even a single donor atom located in a suitable point of the elementary cell) or larger precipitates in the shape of a parallelepiped with the following edges: [110], [1$\bar{1}$0] and [001]. For the time being, experimental data, giving information about the core of the defects, are lacking, so the simulations were performed using the point-defect model. A uniform defect distribution was assumed (therefore, the correlation function was neglected). If these defects were pairs of Te atoms, the same results could be obtained by treating the defects as single atoms and taking into account the correlation functions describing the pairs. However, if these are many-atom defects, then the description of the measured orthorhombic symmetry of the displacement field in terms of the many-atom correlation function would be very complicated and not useful. On the other hand, treating the whole atomic cluster (single atom, several atoms, or several tens of atoms) as a single defect, one can describe all the mixed situations.

The simulations for the Huang region (Huang 1947) confirm that the displacement field outside the defect has an orthorhombic symmetry. Their size and the force exerted by them on the surrounding lattice can be identical for every single defect or, more probably, they can be statistical quantities. In the latter case the maps and the profiles in the Huang region will not change, but the values of P_{ij} will be replaced by $\langle P_{ij} \rangle$, and the oscillations in the Stokes–Wilson region (Borowski & Gronkowski 1999) will be smeared out (averaged), leading to the dependence $I_{\mathrm{D}}(q) = C/q^{\alpha}$, α being dependent on the distribution of the defect sizes, and C being a constant. However, for the time being, measurements in this region are lacking.

4. Conclusions

This paper presents the method of measuring X-ray diffuse-radiation intensity for characterization of defects formed as a result of various technological processes in GaAs crystals doped with Te.

It is stressed that a statistical distribution of defects consisting of many atoms can be described in two ways: either it can be treated as a uniform distribution of many-atom defects, or a non-uniform distribution of single-atom defects (obviously, in some cases non-uniform distributions of many-atom defects are also measured, (see, for example, Kaganer *et al*. 1997)).

Using the example of the dislocation-loop and orthorhombic-defect formation processes in GaAs, the influence of the amount of diffuse scattering on the measured maps of intensity is demonstrated.

The present work was done within the grant T08A 027 15 of the State Committee for Scientific Research (KBN).

References

Borowski, J. 1997 *Comp. Mater. Sci.* **8**, 261.

Borowski, J. 1998 PhD dissertation, University of Warsaw (in Polish).

Borowski, J. & Gronkowski, J. 1999 *J. Alloys Compounds* **286**, 250.

Borowski, J., Gronkowski, J., Zielińska-Rohozińska, E. & Słupiński, T. 1998 *J. Phys.* D **31**, 188.

Dederichs, P. H. 1971 *Phys. Rev.* B **4**, 1041.

Feller, W. 1961 *An introduction to probability theory and its applications.* Wiley.

Fuller, C. G. & Wolfstrin, K. B. 1963 *J. Appl. Phys.* **34**, 2287.

Holý, V. & Mikulik, P. 1996 *X-ray and neutron dynamical diffraction* (ed. A. Authier, S. Lagomarsino & B. K. Tanner). NATO ASI Series B, vol. 357, p. 259.

Huang, K. 1947 *Proc. R. Soc. Lond.* A **190**, 122.

Kaganer, V. M., Köhler, R., Schmidbauer, M., Opitz, R. & Jenichen, B. 1997 *Phys. Rev.* B **55**, 1793.

Krivoglaz, M. A. 1984 *Diffuznoye rasseyanye rentgenovskich luchey i neytronov na fluktuacyonnych neodnorodnostyach v nieidealnych kristalah.* Kiev: Naukova Dumka.

Kubo, R. 1962 *J. Phys. Soc. Japan* **17**, 1101.

Lang, A. R. 1957 *Acta Metall.* **5**, 358.

Lang, A. R. 1959 *Acta Crystallogr.* **12**, 249.

Larson, B. C. & Schmatz, W. 1974 *Phys. Rev.* B **10**, 2307.

Levine, M. J. & Wright, J. 1971 *Phys. Rev. Lett.* **26**, 1351.

Słupiński, T., Zielińska-Rohozińska, E. & Harasimowicz, T. 1996 *Acta Phys. Polon.* **90**, 1080.

Trinkaus, H. 1971 *Z. Angew. Phys.* **31**, 229.

Trinkaus, H. 1972 *Physica Status Solidi* B **51**, 307.

Wesley, J. C. & Rich, A. 1970 *Phys. Rev. Lett.* **24**, 1320.

Zielińska-Rohozińska, E., Słupiński, T., Gronkowski, J., Harasimowicz, T. & Borowski, J. 1997 *Nuovo Cim.* D **19**, 625–635.